

Resistivity and Magneto-Optical Evidence for Variable and Incomplete Connectivity in Dense, High Critical Current Density C-alloyed Magnesium Diboride.

B. J. Senkowicz, A. A. Polyanskii, R. J. Mungall, E. E. Hellstrom, and D. C. Larbalestier

*Applied Superconductivity Center and Department of Materials Science and Engineering,
University of Wisconsin – Madison, Madison, WI 53706*

Carbon-doped magnesium diboride was fabricated from pre-reacted pure MgB₂ by mechanical alloying. The sample set had excellent critical current densities $J_c(8\text{ T}, 4.2\text{ K})$ ranging from 15 – 60 kA/cm², depending on composition. Magneto-optical imaging detected regions up to 0.5 mm in size which were ~100% dense with J_c 2-6 times that of the matrix. Evaluation of resistivity curves using the Rowell method predicts that only 10-50% of the cross sectional area carries the normal state measurement current, suggesting that considerable increases in J_c in these ~80% dense MgB₂ samples would be possible with complete grain and particle connectivity.

The fabrication of MgB₂ wires in lengths > 1 km and in stabilized multifilamentary form¹⁻³ demonstrates that this is a conductor technology of great interest to magnet builders.⁴ But to make MgB₂ really viable, the critical current density J_c must be raised considerably. A useful near-term benchmark would be to make J_c better than NbTi. For example at 8 T and 4.2 K, this would imply an increase in J_c by a factor of 3-5. This letter addresses the important obstacle of less than full connectivity that stands in the way of achieving this goal.

Most practical superconductors achieve $J_c \sim 10\%$ of the depairing current density $J_d \sim H_c/\lambda$, where H_c is the thermodynamic critical field ($\mu_0 H_c \sim 0.67$ T) and λ is the London penetration depth (~ 140 nm), which yields $J_d(4.2\text{ K}) \sim 4 \times 10^8$ A/cm². But in fact few bulk MgB₂ samples attain even 10^6 A/cm²⁻⁵. However, $J_c \sim 10^7$ A/cm² has been obtained in clean, undoped MgB₂ films grown by hybrid physical – chemical vapor deposition (HPCVD)⁶. Such films appear to have almost perfect connectivity, but their disadvantage is that they have low H_{c2} and J_c decreases rapidly with increasing applied field. C-doped HPCVD films have much higher H_{c2} but J_c is much lower due to current blockage by non-superconducting carbon-rich phases.⁶ Currently, the best⁷⁻¹¹ reported C-doped bulk MgB₂ has $J_c(8\text{ T}, 4.2\text{ K})$ in the range of 20 – 60 kA/cm². Like the C-doped films, bulk MgB₂ suffers from obstructed current flow, as described by Rowell.¹² This sub-optimal electrical connectivity is usually ascribed to a combination of porosity and grain boundary wetting phases¹²⁻¹⁴, but the real reason is seldom clear. If poor connectivity is as general as the Rowell analysis predicts, in fact the intragranular J_c of much bulk MgB₂ may already be higher than of Nb-Ti. This letter provides support for this view from a systematic study of connectivity in bulk MgB₂ which demonstrates that local variations of at least 3 in the current-carrying cross-section and/or the local J_c value occur, even in high J_c MgB₂.

Our sample set had compositions $\text{Mg}(\text{B}_{1-x}\text{C}_x)_2$, with X ranging from 0 to 0.1. Precursor powders of MgB_2 , Mg , and C were mixed in stoichiometric proportions and mechanically alloyed in a SPEX mill with WC media for 600 min. Milled powders were then pressed into pellets, sealed in evacuated stainless steel tubes, and reacted in a hot isostatic press at ~ 0.2 GPa and 1000°C for 200 min followed by a 30 min ramp to 900°C for 300 min and then cooled at a rate of $\sim 100^\circ\text{C/hr}$. Samples sectioned with a diamond saw were $\sim 80\%$ dense and lustrous when polished.

Zero-field cooled, warming T_c transitions were quite sharp at low X , but beyond $X \sim 0.07$ broadened considerably and the higher T onset of the transition stopped decreasing. These characteristics indicate some inhomogeneity in carbon alloying beyond $X \sim 0.07$.¹⁵ However, we did not observe a double transition in any of the samples, which would have indicated phase separation.

Figure 1 shows images of a polished ~ 110 μm thick section of the $X = 0.1$ sample, first by conventional light microscopy and then by magneto-optical (MO) imaging in the superconducting state. Both techniques show that the microstructure is inhomogeneous. Fig. 1a shows bright, highly reflective “islands” ranging in size from a few to >100 μm embedded in a duller, more porous matrix. Similar morphology was observed for all $X \geq 0.01$. The fine microstructure is not accessible to the light microscope and is currently being studied by electron microscopy. The MO images of this same piece in Fig 1b show that polishing to thin sections did produce some large cracks, but more significantly that many of the bright islands in Fig. 1a correlate directly to important features in the MO image, as particularly noted by the three islands marked by arrows. The large MO image shows the sample after zero-field cooling to 10 K and then after applying 80 mT, which is not high enough to penetrate the whole sample.

The small dark spots visible in the large MO image correspond to dense islands. The dark MO contrast of the islands indicates that they preferentially exclude flux compared to the matrix around them. The higher field (120 mT) inset MO image in Fig. 1b shows field penetrating the whole sample. The flux gradient was measured along line C-D and found to be at least 3 times steeper in the island compared to the matrix. Other islands (including those marked by the arrows) had 2-6 times larger gradients than that of the matrix, indicating a proportional variation of J_c .

Using scanning electron microscopy we found substantial porosity in the matrix, but almost full density in the islands, as shown in Fig 2. The near absence of porosity in Fig. 2b is a rare example of complete sintering and densification in C-doped MgB_2 powder without adding Mg from outside the pellet.

The Rowell analysis¹² provides a means to estimate the fraction (A_F) of the sample cross section that carries the current in a normal-state resistivity measurement ($\rho(T)$). Assuming that fully connected pure MgB_2 has a well defined scattering that yields a characteristic $\Delta\rho = \rho(300\text{ K}) - \rho(>T_c)$ regardless of fabrication process, it is possible to separate the effects of electron scattering from connectivity on the normal state $\rho(T)$ curve and thus calculate the true resistivity of the connected portion of the sample, which Rowell called $\rho(0)$ and we call the adjusted resistivity (ρ_A). However, in this study we also need to account for the extra scattering produced by C to make realistic estimates of A_F . To do this we used $\Delta\rho$ data taken on dense C-doped filaments¹⁶⁻¹⁷.

Figure 3 gives measured $\rho(40\text{K})$, $\rho_A(40\text{ K})$, and A_F values for the sample set. Resistivity values vary over about two orders of magnitude and have a large scatter, but do show a general increase with increasing X. Despite the wide scatter in the measured $\rho(40\text{ K})$, the adjusted true

resistivity $\rho_A(40\text{ K})$ is a smooth increasing function of X , indicating that sample-to-sample variation in connectivity is well accounted for by the Rowell analysis. Calculated A_F values are widely scattered and range from ~ 0.14 to ~ 0.50 , indicating that electrical connectivity is significantly impeded, even in these $\sim 80\%$ dense samples. In fact the modeling of current flow in superconductors shows that physical obstructions to the current flow are significantly larger than in the normal state due to the highly non-linear voltage-current characteristics, making it clear that the local J_c will be higher than simply dividing the critical current by A_F .¹⁸ It should be stressed that although high density is beneficial to electrical connectivity, even a fully dense sample could have poor connectivity due to wetting grain boundary phases.

Figure 4 shows whole-sample J_c values calculated from magnetization loops taken in a vibrating sample magnetometer (VSM) on rectangular section bars using the Bean model formula $M=J_c d((3b-d)/d^2)$ where b and d are the sample dimensions perpendicular to the applied field. Uncertainty in b and d was probably $\sim 10\%$. For this sample ($X = 0.1$), $J_c(0\text{T and } 8\text{ T at } 4.2\text{ K})$ was ~ 200 and $\sim 15\text{ kA/cm}^2$, respectively, while for other compositions $J_c(8\text{T, } 4.2\text{K})$ was as high as $\sim 60\text{ kA/cm}^2$, amongst the highest J_c values found in bulk samples. Consistent with our earlier comment, a $J_c(0\text{T, } 4.2\text{K})$ of $\sim 200\text{ kA/cm}^2$ is rather low, only $0.005 J_d$.

From the flux gradients observed by MO along line C-D in Fig. 1b, we calculated the local J_c of the matrix and an island.¹⁹ The inset to Fig. 4 compares $J_c(T)$ of the matrix estimated from the MO images with the VSM data. Their close agreement indicates that the VSM-derived J_c values are determined by the whole-sample matrix currents. We found J_c of the islands to be 2 to 6 times higher than that of the matrix, suggesting that full densification is an important route to raising J_c in practical forms of alloyed MgB_2 . At present their effect on the whole sample J_c is limited because the islands are disconnected from each other.

In summary, these dense, hot isostatic pressed high J_c samples were found to be much denser than normal samples²⁰ but still physically and electrically inhomogeneous. Although possessing an already high J_c for bulk samples, significantly higher J_c islands of almost full density surrounded by a lower J_c , ~80% dense matrix were observed. Rowell connectivity analysis predicted that the X=0.1 sample had an effective cross section of only ~0.3 for normal state currents flowing across the matrix. This reduced A_F factor suggests at least a factor of 3 increase in local flux pinning current density, a result which is broadly consistent with the 2 to 6 times higher local current density of fully dense regions indicated by MO flux gradient measurements. Thus it is clear that one path to obtaining higher current densities in MgB₂ that are comparable to Nb-Ti is to fully densify the material. Further densification experiments are underway to check this conjecture.

BJS was supported by the Fusion Energy Sciences Fellowship Program, administered by Oak Ridge Institute for Science and Education under a contract between the U.S. Department of Energy and the Oak Ridge Associated Universities. This work was supported by the NSF – FRG on MgB₂, and by DOE – Understanding and Development of High Field Superconductors for Fusion - DE-FG02-86ER52131. The authors thank their Madison colleagues J. Jiang, W. Starch, A. Squitieri, and J. Mantei and visiting scientists in Madison, A. Matsumoto of NIMS, and A. Yamamoto of the University of Tokyo for discussions.

1. A. Stenvall, A. Korpela, R. Mikkonen and G. Grasso. Supercond Sci Technol, **19**, 184-9 (2006).
2. R. Musenich, P. Fabbriatore and S. Farinon, et al. IEEE Trans. Appl. Supercond., **15**, 1452-6 (2005).
3. M.D. Sumption, M. Bhatia and F. Buta, et al. Supercond Sci Technol, **18**, 961-5 (2005).
4. Y. Iwasa, D.C. Larbalestier, M. Okada, R. Penco, M.D. Sumption and X.X. Xi. IEEE Trans App Sup, **To Be Published**, (2006).
5. Ueda, J. Shimoyama and A. Yamamoto, et al. Physica C, **426-431**, 1225-30 (2005).
6. A.V. Pogrebnyakov, X.X. Xi and J.M. Redwing, et al. Appl. Phys. Lett., **85**, 2017-9 (2004).
7. B.J. Senkowicz, J.E. Giencke, S. Patnaik, C.B. Eom, E.E. Hellstrom and D.C. Larbalestier. Appl. Phys. Lett., **86**, 202502-1 (2005).
8. A. Matsumoto, H. Kumakura, H. Kitaguchi and H. Hatakeyama. Supercond Sci Technol, **17**, 319-23 (2004).
9. S.X. Dou, V. Braccini and S. Soltanian, et al. J. Appl. Phys., **96**, 7549-55 (2004).
10. M.D. Sumption, M. Bhatia, M. Rindfleisch, M. Tomsic and E.W. Collings. Supercond Sci Technol, **19**, 155-60 (2006).
11. H.L. Xu, Y. Feng and Y. Zhao, et al. Superconductor Science and Technology, **19**, 68-71 (2006).
12. J.M. Rowell, Supercond Sci Technol, **16**, 17-27 (2003).
13. J.M. Rowell, S.Y. Xu and X.H. Zeng, et al. Appl. Phys. Lett., **83**, 102-4 (2003).
14. X. Song, V. Braccini and D.C. Larbalestier. J. Mater. Res., **19**, 2245-55 (2004).
15. A.J. Zambano, A.R. Moodenbaugh and L.D. Cooley. Superconductor Science and Technology, **18**, 1411-20 (2005).

16. R.H.T. Wilke, S.L. Bud'ko, P.C. Canfield, D.K. Finnemore, R.J. Suplinskas and S.T. Hannahs. *Physica C*, **424**, 1-16 (2005).
17. R.H.T. Wilke, Personal Communication.
18. M. Friesen and A. Gurevich. *Physical Review B (Condensed Matter)*, **63**, 064521-1 (2001).
19. A.A. Polyanskii, D.M. Feldmann and D.C. Larbalestier. C3.4 in *Handbook of Superconducting Materials*. Edited by D. Cardwell and D. Ginley. IOP publishing Ltd., 2003.
20. N.A. Frederick, S. Li, M.B. Maple, V.F. Nesterenko and S.S. Indrakanti. *Physica C*, **363**, 1-5 (2001).

Figure 1 – a) Optical image of a polished thin section with $X = 0.1$. b) Magneto – optical (MO) images of the same sample. Large MO image was zero-field cooled to 10 K , then 80 mT was applied. Cracks are marked with “X” Inset MO image was zero-field cooled to 10 K before 120 mT was applied.

Figure 2 – Secondary electron micrographs of the $X = 0.1$ sample fracture surface. a) Representative porous matrix. The brightness is due to the high density of edges within the microstructure. b) Representative dense island.

Figure 3 – Measured $\rho(40\text{ K})$, calculated $\rho_A(40\text{ K})$ and calculated A_F as a function of nominal composition using $\Delta\rho$ data taken from dense, low-resistivity, carbon doped filaments.¹⁷

Figure 4 – VSM J_c as a function of applied field at a variety of temperatures for $X = 0.1$. Inset shows J_c as a function of temperature for $X = 0.1$ at low field as measured by VSM (open squares) and as reconstructed from flux penetration gradients across the *matrix area* along line C-D in Fig. 1b measured by MO with $H < 200\text{ mT}$.

Figure 1

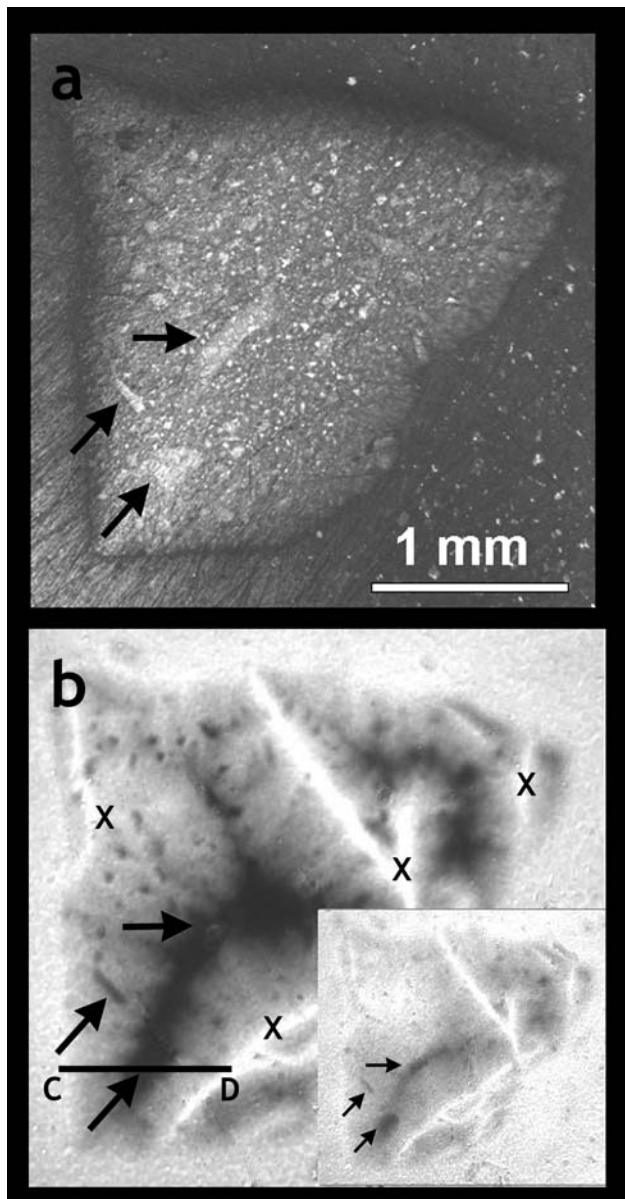


Figure 1

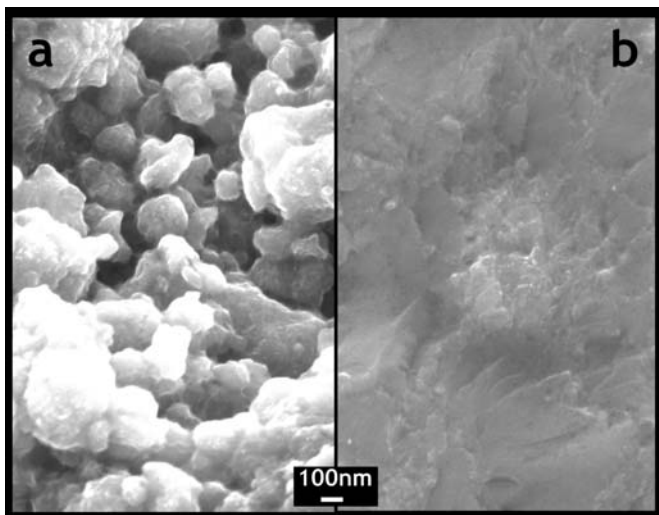


Figure 3

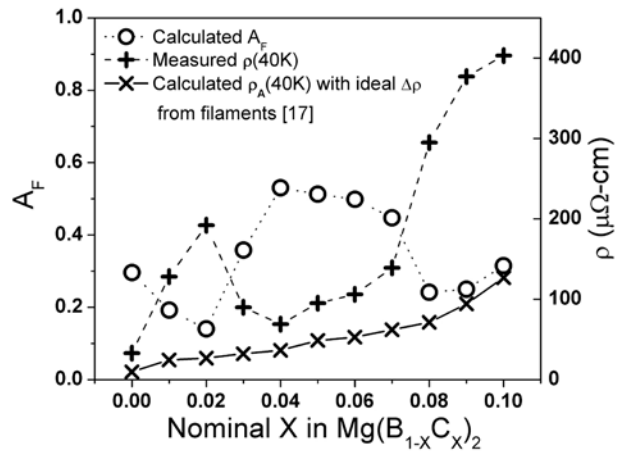


Figure 4

